

Dissolved Fe^{2+} and $\sum\text{H}_2\text{S}$ Behavior in Sediments Seasonally Overlain by Hypoxic-to-anoxic Waters as Determined by CSV Microelectrodes

KAREN S. SELL^{1,★} and JOHN W. MORSE²

¹*Department of Geology & Geophysics, Texas A&M University, College Station, Texas, 77843, USA;* ²*Department of Oceanography, Texas A&M University, College Station, Texas, 77843, USA*

Received 27 April 2005; accepted 31 October 2005

Abstract. Variability of dissolved Fe^{2+} and $\sum\text{H}_2\text{S}$ concentrations in porewaters were studied, using cathodic stripping voltammetry (CSV) microelectrodes, in sediments overlain by hypoxic waters in the summer from the southeastern region of Corpus Christi Bay, Texas (CCB) and the Mississippi River Bight (MRB), Louisiana. These measurements were complimented by sediment microcosm studies where oxygen concentrations in the overlying water were manipulated. Sulfate reduction rates, benthic oxygen demand, total reduced sulfide, porewater sulfate, and total organic carbon were also determined. Fe^{2+} and $\sum\text{H}_2\text{S}$ were the major dissolved redox-reactive dissolved species in these sediments. During hypoxic conditions, an upward migration of porewater Fe^{2+} and $\sum\text{H}_2\text{S}$ occurred, with Fe^{2+} reaching much higher maximum concentrations than $\sum\text{H}_2\text{S}$. Statistically significant ($p < 0.05$) differences in both Fe^{2+} and $\sum\text{H}_2\text{S}$ occurred between sediments at the CCB and MRB study sites. Although both sites were Fe-dominated, reactive and dissolved iron were higher while $\sum\text{H}_2\text{S}$ was lower at the MRB site. However, there were no statistically significant ($p > 0.05$) difference in regard to $\sum\text{H}_2\text{S}$ between microcosm and field monitoring studies. Results indicated that, for Fe^{2+} and $\sum\text{H}_2\text{S}$, relatively large and rapid changes occurred in both the concentrations and distributions of these important porewater constituents in response to relatively short-term changes in overlying water oxygen content. Model calculations indicated that conditions in the sediments can be responsible for the induction of hypoxic conditions in the formation of hypoxic overlying waters in <6 days at CCB and ~20 days at MRB.

Key words: benthic oxygen demand, hypoxia, microelectrodes, porewater iron and sulfide, sedimentary biogeochemistry

1. Introduction

Most previous studies of benthic biogeochemical processes in seasonally hypoxic ($<2 \text{ mg O}_2 \text{ L}^{-1}$ or $<63 \mu\text{M}$) areas generally are focused on dissolved sulfide generation and release from sediments into the overlying bottom waters because of sulfide toxicity to organisms (Jørgensen et al., 1990; Roden

★ Author for correspondence. E-mail: ksell@neo.tamu.edu

and Tuttle, 1992; Cooper and Morse, 1996). During a hypoxic event, the release of H_2S into the bottom waters can cause the surrounding organisms to be poisoned by sulfide through diffusion into their skin where oxidative enzymes are blocked causing suffocation (Theirmann et al., 2000). Therefore, few benthic animals are able to tolerate the physiological stress associated with extended exposure to low oxygen conditions (Jørgenson, 1980; Harper et al., 1981; Ritter and Montagna, 1999). Some direct effects of low oxygen include reduced benthic abundance, biomass, and diversity, avoidance by mobile fauna, emergence of infauna, and death (Dauer and Ranasinghe, 1992; Buzzelli et al., 2002). Hypoxia can even affect higher trophic levels by decreasing the available prey, where commercial and recreational fishery stocks may be disturbed.

Dissolved Fe^{2+} in sediments underlying hypoxic and anoxic waters has received less attention than sulfide because it is usually at much lower concentrations than dissolved sulfide. However, the study of dissolved Fe^{2+} in sediments underlying hypoxic and anoxic waters is also essential because, even when its concentration is low, it can play an important role by reacting with sulfide to form iron-sulfide minerals (e.g., FeS , pyrite), preventing sulfide release into the overlying waters (e.g., Wilkin and Barnes, 1997). A number of studies over the last decade have been focused on the Fe and S dynamics at the sediment–water interface of marine sediments. Results from such studies indicate that although the majority of the dissolved sulfide reacts with iron to form Fe–S minerals, less than 30% is permanently buried because of re-oxidation, (e.g., Thamdrup et al., 1994; Jørgenson et al., 1990). Under hypoxic to anoxic conditions the oxidation of sulfide can only occur through iron minerals such as Fe_2O_3 , since dissolved oxygen is not readily available. Although some studies indicate that sulfide can be released to overlying waters during hypoxic to anoxic bottom water conditions (Roden and Tuttle, 1992; Cooper and Morse, 1996; Luther et al., 2004), others report that the sediments are able to prevent the upward diffusion of sulfide through the formation of Fe–S minerals under such conditions (e.g., Kristiansen et al., 2002). These recent studies have consequently emphasized the need to gain better knowledge of the temporal behavior of both the sedimentary Fe and S pools under low oxygen conditions in a variety of marine sediments and bays.

The objective of this study was to determine and compare the behavior of dissolved Fe^{2+} and $\sum\text{H}_2\text{S}$ concentrations in sediment porewaters from seasonally hypoxic coastal areas on the Gulf of Mexico to obtain a better understanding of their responses to changing oxygen concentrations in the overlying water. Sediments from two seasonally hypoxic coastal environments, Corpus Christi Bay, Texas (CCB) and the Mississippi River Bight, Louisiana (MRB), were investigated. At CCB observations were made

from both freshly collected cores and through manipulation of overlying water oxygen in microcosms. At MRB observations were made only with the use of microcosm studies. Dissolved Fe^{2+} and $\sum\text{H}_2\text{S}$ concentrations were determined using CSV microelectrodes (Brendel and Luther, 1995; Luther et al., 1998) to produce fine-scale depth profiles in a non-destructive manner. Traditional techniques for determination of sulfate reduction rates (SRR), benthic oxygen demand (BOD), total reduced sulfide (TRS), porewater sulfate, and total organic carbon (TOC) supplemented micro-electrode measurements and allowed further comparison of the two study sites.

2. Study sites

Hypoxia can occur via the combination of two principle mechanisms: (1) stratification of the water column and (2) consumption of oxygen by decomposition of organic matter. Further contributors to hypoxia can include increased temperatures during the summer months that can increase the benthic metabolism and thermal stratification, and increased nutrient loads from river runoff that can deplete oxygen levels by enhancing surface primary production and the supply of organic material to the hypoxic water column and sediments.

Most Texas bays are shallow (typically $\sim 1\text{--}2$ m) with common wind and storm events, as well as tidal flushing that promote mixing and exchange with coastal waters. Consequently, Texas bays would not seem likely regions for hypoxic episodes. However, summer hypoxic events have been reported to occur in several locales. A well-known area includes Corpus Christi Bay (e.g., Ritter and Montagna, 1999). In CCB hypoxic events occur during the summer months of July and August. This is when salinity stratification is greatest and temperature is highest due to increased solar radiation (Ritter and Montagna, 1999). The occurrence of acute hypoxia in the southeastern region of this shallow (~ 2 m) bay implies that benthic processes may play an important role due to the low overlying water volume to benthic surface area ratio ($\sim 2000 \text{ dm}^3 \text{ m}^{-2}$), where the impact of reduced components and resulting oxygen consumption from the sediments may be greatest. The CCB sampling sites are shown in Figure 1.

Summer hypoxia has also been observed on the inner continental shelf of the northwest Gulf of Mexico west of the Mississippi River Delta (the “dead zone”) over the last century (Rabalais et al., 1994, 2002; Rowe, 2001; Stow et al., 2005). This area is significantly deeper ($\sim 5\text{--}60$ m) than the Corpus Christi Bay site and hypoxia persists below the pycnocline because of freshwater run-off from the Mississippi River. Samples were taken from the “dead zone” of the MRB at latitude 28.9760 N and longitude 89.4730 W at a depth of 18 m.

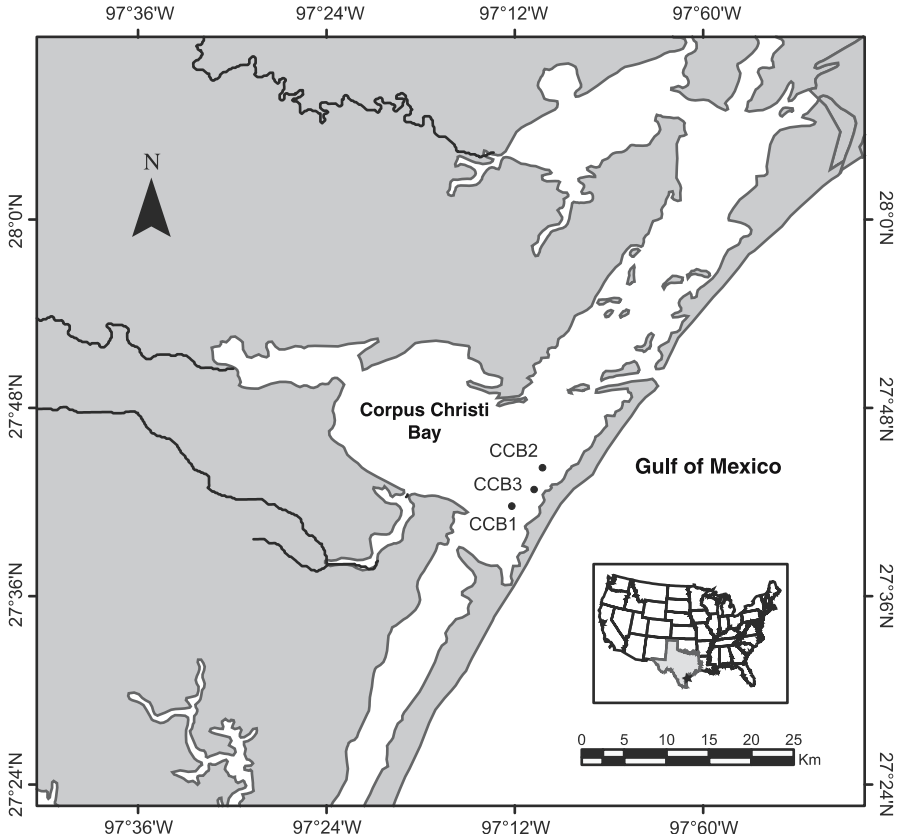


Figure 1. Map of Corpus Christi Bay, Texas and the three study locations.

3. Materials and methods

3.1. SAMPLE COLLECTION

Samples were taken from CCB during a 5-week-period in mid-July to mid-August in the summer of 2002 when hypoxic conditions persisted. Sediment cores were collected manually by SCUBA divers with care to minimize sediment disturbance during the collection activities. After recovery, the cores were promptly covered and clasped with fitted tops and immediately taken to the laboratory for further analyses. Several cores from each site were retrieved as close as possible to one another (~1 m) while taking care to not collect samples from previously cored sediments.

Cores that were taken from each of three sites (Figure 1) included:

- (1) two (one for experimental manipulation and a control) 16 cm diameter and 40 cm-long Plexiglas incubation cores for microelectrode measurements,

- (2) a 2 cm diameter, 30 cm-long Plexiglas core for sulfate reduction rates (SRR) that had injection ports every 2 cm,
- (3) a 7 cm diameter, 40 cm-long Plexiglas core for total organic carbon (TOC), porewater sulfate, and total reduced sulfides (TRS),
- (4) several 7 cm diameter, 40 cm-long Plexiglas cores for microelectrode field monitoring, and
- (5) several 8 cm diameter, 20 cm-long Plexiglas cores for benthic oxygen demand (BOD) were also retrieved.

Samples from the MRB were taken during a July 2002 research cruise on the *R/V Gyre*. A single box core (45 cm × 45 cm) was collected from a depth of 18 m. Cores that were taken included the same as 1–3 above for the CCB sites with the exception of TOC measurements.

3.2. LABORATORY PROCEDURES ON EXPERIMENTAL CORES

Concentrations of O_2 , Fe^{2+} , and $\sum H_2S$ in the porewaters of the top 10 cm of sediment and 1 cm of overlying bottom waters were measured by cathodic stripping voltammetry, using solid state amperometric microelectrodes and an Analytical Instrument Systems model DLK-100 voltammetric analyzer (Brendel, 1995; Brendel and Luther, 1995; Luther et al., 1998). Measurements were made with an Au/Hg amalgam glass microelectrode. Instrumental parameters for the linear sweep and cyclic voltammetry modes were typically 200 mV s⁻¹ scan rate over the potential range -0.1 to -1.8 V with a 10 s deposition at -0.1 V. Minimum detection limits for O_2 , Fe^{2+} and $\sum H_2S$ were approximately 5, 40, and 1 μM . Calibration of each electrode was based on the pilot ion method where Mn^{2+} was the standardized ion (Brendel, 1995). Electrodes were only used if their Mn^{2+} slope was comparable (± 0.2) to the previous work of Brendel (slope = 0.7). After measurements were taken, peak heights were determined automatically through a Labview[®] program where a second derivative baseline fit was made on the voltammograms, following closely Peakfit[®] software. Millimeter scale depth resolution intervals were obtained using a micromanipulator. An advantage to using microelectrodes over traditional methods is that microelectrodes do not seriously disrupt the sediment and the measurement of dissolved concentrations can be obtained on a finer scale than generally possible with other techniques. It is also possible to make repeated profiles on a single core. A typical voltammogram produced in this study is shown in Figure 2 where the Fe^{2+} peak is located at -1.65 V and the $\sum H_2S$ is located at -0.58 V.

The sediment cores for microelectrode analyses were sealed and overlying water aerated with a simple aquarium air pump until the initial electrode measurements were made. Aeration was processed through a hydration flask

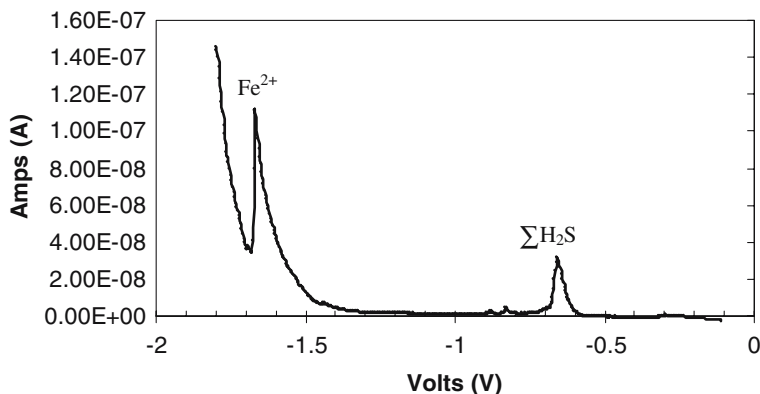


Figure 2. Sample voltammogram (linear sweep mode) from the collected cores indicating Fe^{2+} and $\Sigma\text{H}_2\text{S}$ peaks.

to prevent evaporation of overlying water. The vertical (i.e., down-core) measurement steps were every 1 mm for the first 10 mm and then every 2 mm down to 60 mm, then in steps of 5 mm until 100 mm was reached. Upon completion of the initial survey, aeration was stopped, and the overlying water became hypoxic in the sealed cores. Re-aeration of the core was performed when dissolved redox reactive species were detectable in the overlying water, after approximately 60 hours. Then aeration was terminated once again, after approximately 120 additional hours when the core had reached oxidic ($> 200 \mu\text{M}$) conditions in the overlying water, to induce a “natural” and “short-lived” hypoxic setting.

Electrode profiles were made throughout the entirety of the experiment. Experiment incubation time length varied with site because of different collection times (MRB = ~ 28 days, CCB1 = ~ 21 days, CCB2 = ~ 19 days, CCB3 = ~ 17 days). All profiles were made in different locations in the core to avoid potential error produced by previous electrode penetration and associated small scale core disturbance. Overlying waters were slightly stirred with a small magnet attached to the lid of the microcosm during the experiment and small amounts of mixing occurred during aeration from bubbling. This was done to prevent differences in the benthic boundary layer flow velocity during treatments. Control cores were aerated throughout the experiment entirety and electrode measurements were taken periodically during the experiments. Analysis of all cores was conducted at room temperature (20–22 °C) conditions.

At the CCB sites, dissolved nitrate was present at insignificant concentrations of only a few μM (Gardner, unpublished). Dissolved Mn^{2+} was less than microelectrode detection limits ($< 5 \mu\text{M}$) at both study locations. Consequently, Fe^{2+} and $\Sigma\text{H}_2\text{S}$ were the major redox-reactive species in

sediment porewaters. Cores for BOD at the CCB sites were brought back to the laboratory and were incubated following the method of Lavrentyev et al. (2000) where measurement of the O_2 to Ar ratio in the collected porewater samples was made via mass spectrometry following the method of Kana et al. (1994). TOC at the CCB sites was measured in the top 2 cm of sediments treated with 1 N HCl using a Utopia Instrument Corporation (UIC) carbon furnace and coulometer.

Cores for the determination of SRR at both the MRB and CCB sites were collected, capped, and taken to the laboratory for injection of $10 \mu\text{Ci}$ per injection port of $\text{Na}_2^{35}\text{SO}_4$, then incubated for 24 hours and frozen after the method of Jørgenson (1978). Cores were extruded into 2 cm sections where digestions were done by the boiling Cr(II) + acid method of Canfield et al. (1986) with the exception that the trap solution for the $^{35}\text{H}_2\text{S}$ fraction consisted of Zn-acetate. Both the $^{35}\text{SO}_4^{2-}$ and $^{35}\text{H}_2\text{S}$ fractions were placed into separate scintillation vials with scintillation cocktail and analyzed on a Perkin-Elmer scintillation counter.

The core used for porewater extraction was taken to the laboratory, placed in a glove box under a nitrogen environment in order to prevent oxidation, extruded into 2 cm sections, immediately put on the squeezer rack where sediments were pressurized with N_2 , and porewaters were collected into a syringe attached to the squeezing apparatus. SO_4^{2-} measurements were made on a Dionex ion chromatograph. The remaining sediment cakes were used for solid phase chemical analysis of TOC and TRS. The boiling Cr (II) + acid method (Canfield et al., 1986) and the Cline (1969) H_2S analysis method were used for sulfide extraction and quantification.

3.3. STATISTICAL ANALYSES

Statistical analyses were performed using the SPSS[®] statistical package and the non-parametric Kruskal-Wallis analysis of variance (ANOVA) was chosen because portions of the microelectrode data were not normally distributed ($p > 0.05$), thereby requiring a more conservative statistical approach. Two sets of analyses were made on the collected microelectrode data. The first was a comparison of the Fe^{2+} and $\sum\text{H}_2\text{S}$ depth profiles (-10–50 mm) of averaged triplicate profiles during microcosm studies at CCB and the MRB, and the second was a comparison of the Fe^{2+} and $\sum\text{H}_2\text{S}$ depth profiles (-10–50 mm) of averaged triplicate profiles between field monitoring cores and experimental microcosm incubations at CCB. All statistical analyses were conducted on the entire depth profile for each of the dissolved constituents and not their means because previous literature has suggested that the comparison of concentration averages over an entire depth range is not meaningful (Froelich et al., 1979).

4. Results

4.1. CORPUS CHRISTI BAY FIELD MONITORING STUDIES

During sampling, the surface and bottom water temperature, salinity, and dissolved oxygen (DO) concentrations were measured (Table I). All sites showed relatively little difference in surface and bottom water temperatures (0.5°), but each exhibited salinity stratification (as great as 16) and resulting DO differences (bottom water DO $< 2.5 \text{ mg L}^{-1}$ and surface water DO $\sim 5 \text{ mg L}^{-1}$). The bottom water DO at all stations was hypoxic ($< 2 \text{ mg O}_2 \text{ L}^{-1}$ or $63 \mu\text{M}$) throughout the duration of the study. Over half of the measured DO concentrations in the bottom waters were $< 0.3 \text{ mg L}^{-1}$; indicating severe hypoxia to anoxia. The oxygen penetration depth in the sediments, as measured by microelectrodes, was 8–10 mm. Figure 3 illustrates triplicate depth profiles (–10–50 mm). Maximum dissolved Fe^{2+} concentrations in July and August exceeded those of the $\sum\text{H}_2\text{S}$ by approximately a factor of 30 and Fe^{2+} was measured in the overlying water column during both months.

4.2. CORPUS CHRISTI BAY EXPERIMENTAL MICROCOSM RESULTS

A light brown surface layer was initially present and decreased in thickness during induced hypoxic conditions from $\sim 2 \text{ mm}$ to $\sim 0.5 \text{ mm}$ in thickness.

Table I. CCB and MRB monitored sites temperature (T), salinity, and dissolved oxygen (DO)

Site	Date	T ($^\circ\text{C}$)		Salinity		DO (mg L^{-1})	
		Surface	Bottom	Surface	Bottom	Surface	Bottom
CCB1	19 Jul 2002	29.1	28.9	37.1	40.9	4.80	1.82
CCB1	24 Jul 2002	29.1	29.5	34.1	38.4	4.90	0.10
CCB1	29 Jul 2002	29.4	29.6	30.4	41.6	5.36	0.09
CCB1	5 Aug 2002	29.7	30.2	22.3	26.4	6.79	0.18
CCB1	12 Aug 2002	29.8	30.2	22.8	26.3	5.87	0.11
CCB2	23 Jul 2002	29.1	29.7	28.6	35.4	6.70	0.23
CCB2	29 Jul 2002	29.7	29.3	26.6	28.6	5.82	0.18
CCB2	5 Aug 2002	29.8	30.3	21.9	27.7	7.11	1.01
CCB2	12 Aug 2002	30.0	29.6	21.2	24.5	5.55	2.32
CCB3	29 July 2002	29.7	29.6	27.8	42.9	6.36	0.06
CCB3	5 Aug 2002	29.9	30.1	21.8	28.1	7.10	0.14
CCB3	12 Aug 2002	29.8	29.9	23.0	26.3	5.08	0.52
MRB ^a	7 July 2002	31.4	27.6	25.1	34.8	7.32	0.45

^aMRB data provided by Nancy Rabalais, LUMCON, unpublished.

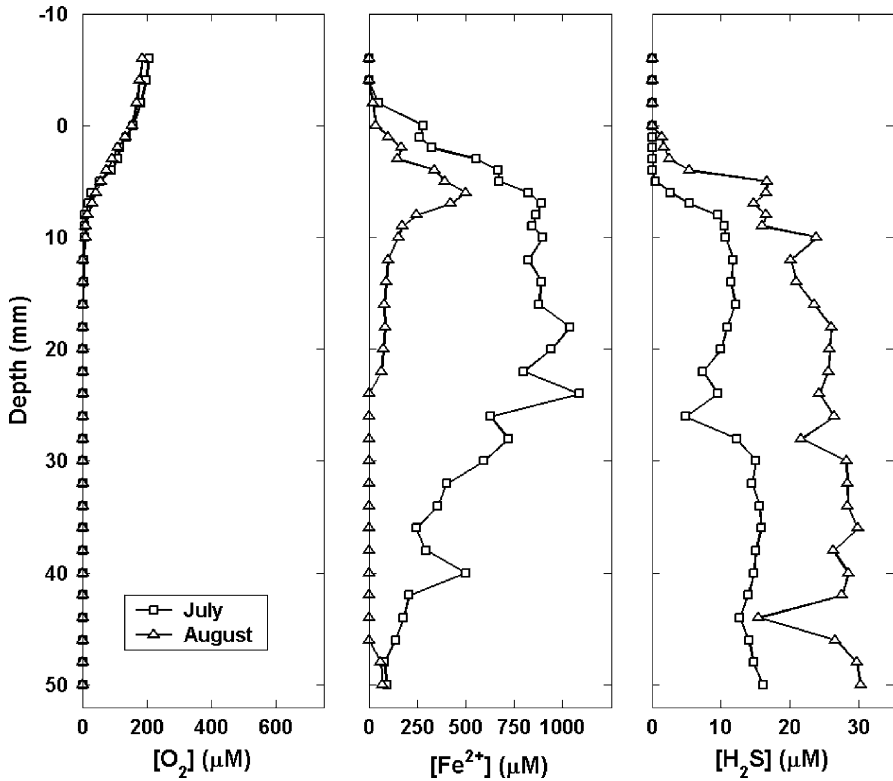


Figure 3. CCB sediment depth profiles of porewater O_2 , Fe^{2+} , and $\sum H_2S$ for July and August. Each point represents triplicate microelectrode measurements at the given depth and oxygen concentration.

Deeper sediments also changed in color from grey–brown to black under decreased DO concentrations. Initially, the sediments appeared to have many (unquantified) burrows indicating the presence of abundant bioturbating macrofaunal organisms. During the on-set of hypoxia, the benthic biota (e.g., polychaetes) migrated into the overlying water, leaving the burrows apparently abandoned.

Figures 4 and 5 present the average of triplicate depth profiles for increasing overlying bottom water DO concentrations. Matlab[®] software was used to linearly interpolate between data points to provide Fe^{2+} and $\sum H_2S$ concentration gradients for different overlying water DO concentrations. At the higher overlying water DO concentrations the depth profiles of dissolved Fe^{2+} and $\sum H_2S$ moved deeper into the sediment, but under hypoxic/anoxic conditions both dissolved Fe^{2+} and $\sum H_2S$ penetrated into the overlying waters. The distributions of dissolved Fe^{2+} and $\sum H_2S$ with sediment depth followed the common redox zonation, where the highest Fe^{2+} concentrations occurred above (2 and 20 mm) the $\sum H_2S$ maximum values (20 and 50 mm).

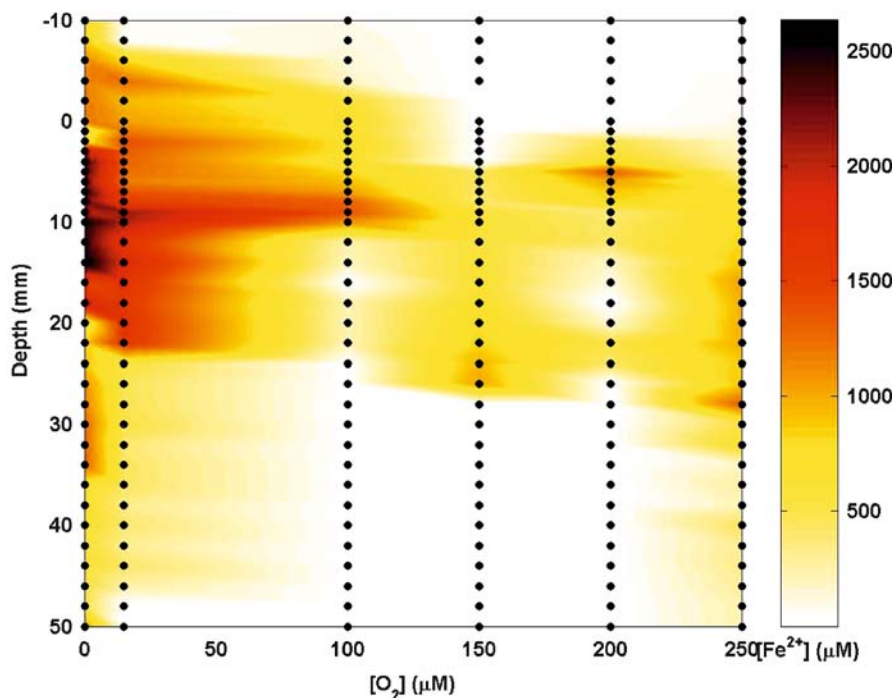


Figure 4. CCB sediment porewater Fe^{2+} concentrations with increasing bottom water DO concentrations. Each point represents triplicate microelectrode measurements at the given depth and oxygen concentration where Matlab[®] then linearly interpolated between points.

The maximum Fe^{2+} concentrations were up to fifty-times those of $\sum\text{H}_2\text{S}$ ($2500 \mu\text{M}$ versus $50 \mu\text{M}$). ANOVA analysis between field monitoring cores and microcosm incubations yielded no significant ($p > 0.05$) difference for $\sum\text{H}_2\text{S}$ (Table II). However, results indicate that there was a significant ($p < 0.05$) difference between conditions for Fe^{2+} (Table II).

The control cores were maintained at close to oxic conditions with DO values in the overlying waters (10 mm above sediment–water interface) $>200 \mu\text{M}$ (6.4 mg L^{-1}). Within the sediment, where dissolved Fe^{2+} and $\sum\text{H}_2\text{S}$ reached a maximum value, Fe^{2+} and $\sum\text{H}_2\text{S}$ average concentrations were much less than those of experimental cores ($\text{Fe}^{2+} < 300 \mu\text{M}$, $\sum\text{H}_2\text{S} < 5 \mu\text{M}$). Little increase from initial concentrations was noted with time for dissolved Fe^{2+} or $\sum\text{H}_2\text{S}$. No measurable release of either Fe^{2+} or $\sum\text{H}_2\text{S}$ into the overlying waters was found for any control core. The observed changes in the porewater chemistry in the experimental cores were, therefore, likely the result of changes in the oxic-hypoxic conditions in the overlying water.

CCB showed SRR that generally decreased with core depth (Figure 6). Of the three CCB sites, CCB3 had the highest maximum SRR, where it exhibited maximum rates $\sim 3 \text{ mmol SO}_4 \text{ m}^{-2} \text{ day}^{-1}$ greater than CCB1 and CCB2

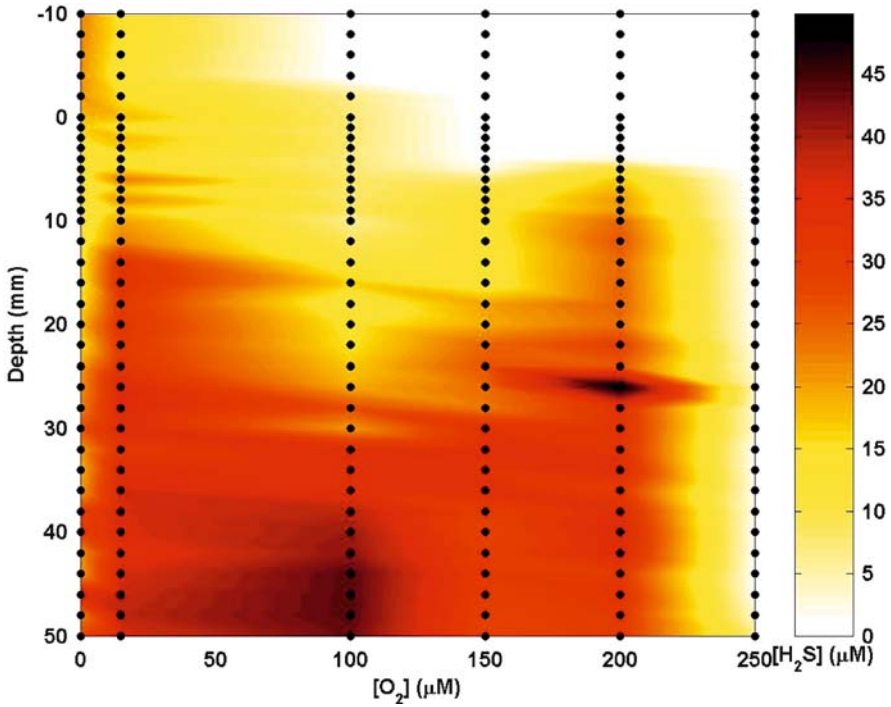


Figure 5. CCB sediment porewater $\Sigma\text{H}_2\text{S}$ concentrations with increasing bottom water DO concentrations. Each point represents triplicate microelectrode measurements at the given depth and oxygen concentration where Matlab[®] then linearly interpolated between points.

Table II. ANOVA results for porewater $\Sigma\text{H}_2\text{S}$ and Fe^{2+} for the CCB field monitoring cores and experimental microcosms

Constituent	ID	N	Rank	Chi-square	Sig. ($p < 0.05$)
$\Sigma\text{H}_2\text{S}$ (μM)	Field Core	108	69.53	2.201	0.138
	Microcosm	36	81.42		
Fe^{2+} (μM)	Field Core	107	79.77	15.300	0.000
	Microcosm	36	48.92		

The entire depth profile of averaged triplicate measurements was used in the ANOVA. Significant differences are indicated ($p < 0.05$).

maximum rates. Further, porewater sulfate, TRS, BOD and TOC were all generally higher at CCB3 (Figure 6 and Table III).

4.3. MISSISSIPPI RIVER BIGHT EXPERIMENTAL MICROCOSM RESULTS

Surface and bottom water temperature, salinity, and DO concentrations at the MRB site were similar to those of the CCB sites (Table I). Figures 7 and 8

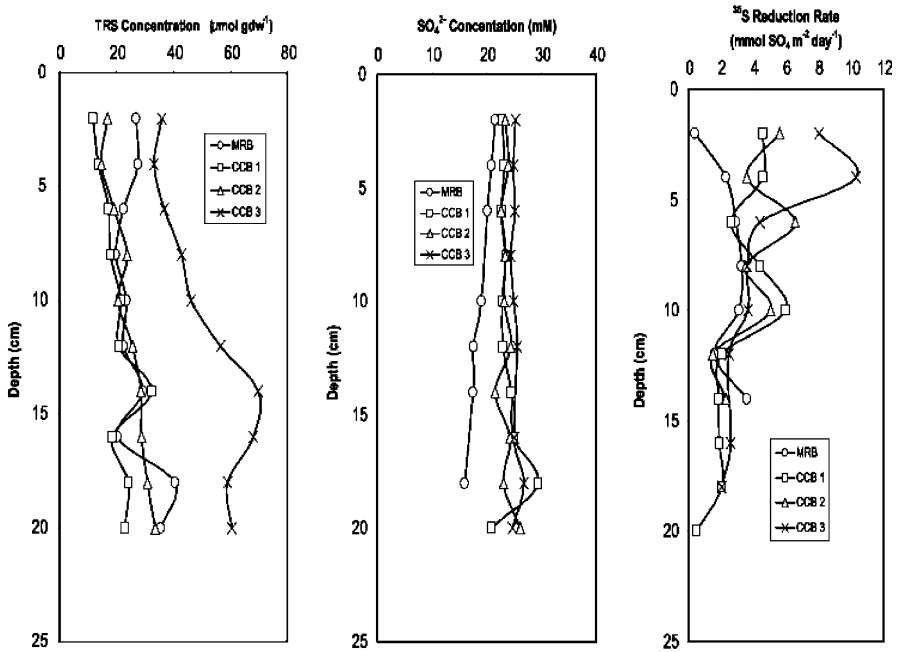


Figure 6. Total reduced sulfides (TRS), porewater sulfate, and sulfate reduction rates (SRR) for CCB and MRB sediments.

Table III. Oxygen demand relationships in the Corpus Christi Bay sediments

Sample	TOC (Dry wt. %)	BOD (mmol O ₂ m ⁻² day ⁻¹)	Integrated SRR (mmol SO ₄ ²⁻ m ⁻² day ⁻¹)	SEOD	R _S
SITE MRB	—	^a 37.50	17.28	1.61	0.9
SITE CCB1	0.22	10.08	23.04	1.92	4.6
SITE CCB2	0.51	17.06	28.80	2.60	3.4
SITE CCB3	0.79	18.36	59.76	4.99	6.5

Total organic carbon (TOC), benthic oxygen demand (BOD), integrated sulfate reduction rate (SRR), sulfide equivalent oxygen demand (SEOD) and the ratio of SEOD to BOD (R_S).

^aData obtained from median MRB values reported by Morse and Rowe (1999).

illustrate the average of triplicate depth profiles at increasing overlying bottom water DO concentrations. Again, Matlab[®] software was used to linearly interpolate between data points to provide Fe²⁺ and \sum H₂S concentration gradients. The responses of dissolved Fe²⁺ and \sum H₂S to changes in overlying water DO content were similar to those observed for the CCB sample. However, the MRB sediments were more Fe²⁺-dominated than the CCB sediments, with Fe²⁺ concentrations approaching 6000 μM whereas \sum H₂S concentrations barely reached 2 μM. ANOVA results comparing Fe²⁺

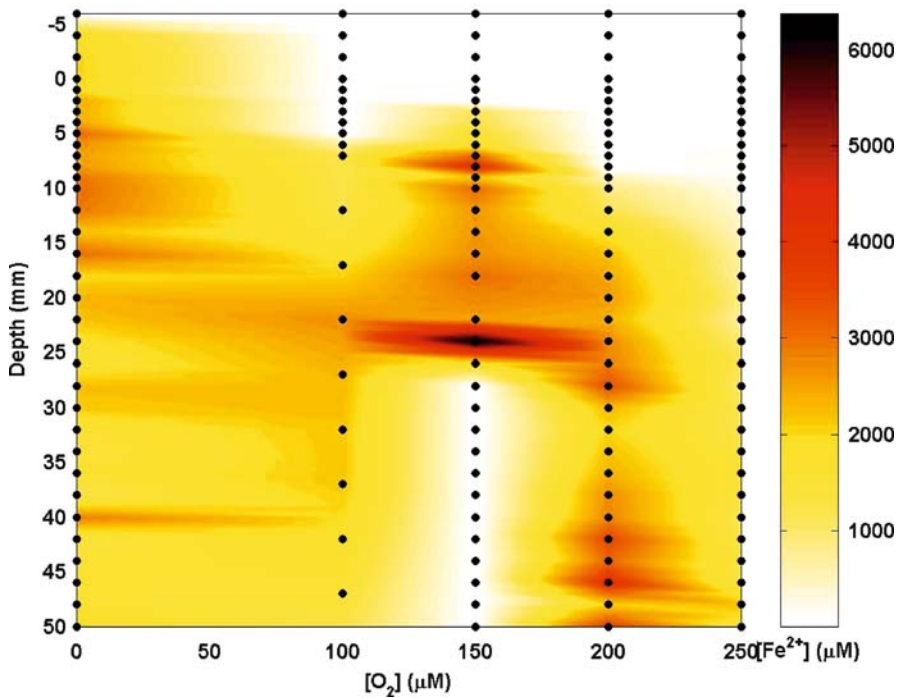


Figure 7. MRB porewater Fe^{2+} concentrations with increasing bottom water DO concentrations. Each point represents triplicate microelectrode measurements at the given depth and oxygen concentration where Matlab[®] then linearly interpolated between points.

and $\sum\text{H}_2\text{S}$ between CCB and the MRB indicate significant ($p < 0.05$) differences in both species (Table IV). Control cores exhibited similar characteristics as the CCB control cores with respect to O_2 , Fe^{2+} and $\sum\text{H}_2\text{S}$. At MRB SRR generally increased with core depth (Figure 6). Sulfate reduction maximum rates at the MRB were $\sim 4 \text{ mmol SO}_4 \text{ m}^{-2} \text{ day}^{-1}$. SRR at CCB were greater than those measured at the MRB, where maximum values reached $\sim 10 \text{ mmol SO}_4 \text{ m}^{-2} \text{ day}^{-1}$. Dissolved sulfate decreased with core depth where minimum concentrations reached 17 mM and TRS ranged from 20 to 40 $\mu\text{mol g dw}^{-1}$ (Figure 6).

5. Discussion

5.1. CORPUS CHRISTI BAY HYPOXIA

5.1.1. Relationship between BOD and SRR

This study of the CCB seasonal hypoxia has provided insight into the impact of hypoxia on the biogeochemistry of the underlying sediments. The concentration of Fe^{2+} in the sediments of this system was vastly greater than that

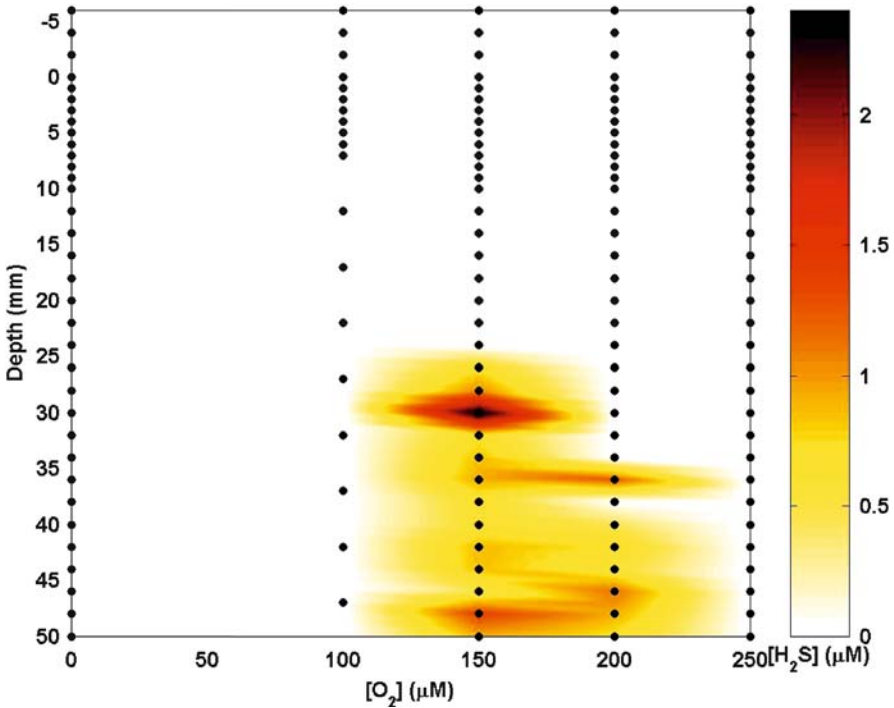


Figure 8. MRB porewater $\Sigma\text{H}_2\text{S}$ concentrations with increasing bottom water DO concentrations. Each point represents triplicate microelectrode measurements at the given depth and oxygen concentration where Matlab[®] then linearly interpolated between points.

of $\Sigma\text{H}_2\text{S}$ during hypoxia and, therefore, based on porewater observations, this region appeared to be dominated by iron reduction relative to sulfate reduction. Additionally, the Fe^{2+} maximum was closer to the sediment–water interface causing Fe^{2+} to be more responsive to changes in the overlying water DO content than $\Sigma\text{H}_2\text{S}$. However, it should be kept in mind that the fractions of both Fe(II) and S(-II) in porewaters is small compared to the total reduced sulfide (TRS) concentration which is dominated by solid phase iron sulfide minerals. Consequently, it is important to examine the changes in porewater concentrations in consideration of this much larger pool of reduced iron and sulfur, as well as the SRR and BOD of the sediments.

The relative importance of the reduced species contribution to maintaining hypoxia can be calculated by considering sulfide and iron behavior. Sulfide will be considered first. It is usually formed in marine waters by the microbial reduction of dissolved sulfate. Three major types of reactions can remove sulfide from porewaters. It can be oxidized by O_2 dominantly through a complex series of bacterial processes or it can be oxidized by reaction with solid phase iron and manganese oxide minerals. Sulfide can also

Table IV. ANOVA results for porewater $\sum\text{H}_2\text{S}$ and Fe^{2+} for the CCB and the MRB microcosm experiments

Constituent	O_2 (μM)	Site	N	Rank	Chi-square	Sig. ($p < 0.05$)
$\sum\text{H}_2\text{S}$ (μM)	0	CCB	34	17.50	58.41	0.000
		MRB	36	52.50		
	100	CCB	20	12.50	32.50	0.000
		MRB	36	37.67		
	150	CCB	34	23.51	24.50	0.000
		MRB	36	46.82		
	200	CCB	34	21.76	33.30	0.000
		MRB	36	48.47		
	250	CCB	34	21.50	39.90	0.000
		MRB	36	48.72		
Fe^{2+} (μM)	0	CCB	34	45.91	17.30	0.000
		MRB	36	25.67		
	100	CCB	20	29.60	0.14	0.706
		MRB	36	27.89		
	150	CCB	33	38.64	3.50	0.063
		MRB	35	30.60		
	200	CCB	34	44.00	12.75	0.000
		MRB	36	27.47		
	250	CCB	34	38.09	1.07	0.301
		MRB	36	33.06		

The entire depth profile of averaged triplicate measurements was used in the ANOVA. Significant differences ($p < 0.05$) between the locations are shown at various bottom water DO concentrations.

be removed from porewaters by the precipitation of iron sulfide minerals. The contribution of sulfate reduction to oxygen removal can be approximately determined from the relationship between measured SRR and BOD. A common practice (see for example Morse and Rowe, 1999) is to calculate the portion of the BOD that is consumed by the oxidation of sulfide and presume that the difference is due to the direct aerobic oxidation of organic matter. Ecologists using this approach often refer to BOD as “net community metabolism”. For anaerobic coastal sediments overlain by oxic waters, this is often a reasonable approximation since commonly >95% of the produced sulfide is oxidized (e.g., Jørgensen, 1977; Berner and Westrich, 1985). A more questionable assumption, which is clearly not valid here for iron, is that oxidation of reduced iron is of negligible importance to BOD.

Integrated SRR and BOD values are presented in Table III, along with the oxygen demand that would be generated by oxidation of the sulfide (sulfide equivalent oxygen demand-SEOD) assuming 2 O_2 are required to

oxidize H_2S to SO_4^{2-} . Usually SEOD is less than BOD. However, under the hypoxic conditions the opposite is true for the sediments in this region where the ratio of SEOD to BOD ranges from 3.7 to 6.5. Although this is not what is usually observed for sediments overlain by oxic waters, it is not surprising for sediments overlain by hypoxic waters because, as the O_2 in the overlying water goes to 0, the apparent (not potential) BOD will also go to zero (see discussion in Morse and Rowe, 1999).

5.1.2. *Iron reduction*

Understanding the behavior of iron is more difficult, because unlike the direct measurement of SRR, there are no reliable methods for directly determining iron oxide reduction rates (see extensive discussion in Thamdrup, 2000). Iron reduction in sediments can take place by two primary mechanisms. These are bacterial reduction of iron oxides or via iron oxide mineral reaction with dissolved sulfide. The Fe(II) produced can accumulate in solution dissolved as Fe^{2+} species, $\text{FeS}_{(\text{aq})}$ clusters and FeS (mackinawite) nanoparticles (e.g., Theberge and Luther, 1997; Morse and Rickard, 2004). The dissolved Fe(II) can be removed by formation of authigenic minerals such as mackinawite, greigite, pyrite, and siderite. Fe^{2+} can also build up in porewaters due to the oxidation of iron sulfide minerals in which the sulfide is preferentially oxidized relative to Fe(II) (Aller, 1980). However, this process was probably not of great importance under the experimental conditions where the overlying waters were close to anoxic. Previous studies of estuarine regions where bacterial iron reduction contributes >16% of the total carbon mineralization indicate that the amount of extractable Fe-oxides range from 10 to $40 \mu\text{mol cm}^{-3}$ ($\sim 23\text{--}91 \mu\text{mol g dw}^{-1}$), using a porosity of 0.8 (Thamdrup, 2000). The concentration of HCl-extractable iron in sediments of CCB is similar ($10\text{--}40 \mu\text{mol g dw}^{-1}$; Sell, 2003) implying that carbon oxidation rates by heterotrophic iron reduction in CCB could also be similar. Further, if the oxidation of sulfide by iron-oxide minerals is considered an important pathway, the contribution to the build-up of Fe^{2+} in porewaters may also be important. The change in porewater Fe^{2+} is approximately equal to the SRR in the CCB sediment; therefore, iron reduction must also be considered important in this Bay.

5.1.3. *Benthic induction of hypoxia*

The rate at which the sediment could induce hypoxia in the overlying water at CCB was calculated using a BOD of $\sim 1 \text{ mmol O}_2 \text{ m}^{-2} \text{ hour}^{-1}$ and letting the bottom water hypoxic thickness to be equal 1 m (Ritter and Montagna, 1999). The conservative BOD value of $\sim 1 \text{ mmol O}_2 \text{ m}^{-2} \text{ hour}^{-1}$ was estimated based on BOD measurement given in Table III; the values measured ($10\text{--}20 \text{ mmol O}_2 \text{ m}^{-2} \text{ day}^{-1}$) were under hypoxic conditions but under oxic

to sub-oxic conditions one would expect values to certainly be greater. The time for onset of hypoxia in a closed system was estimated to be <6 days. However, under oxic-to-sub-oxic conditions where overlying DO values are greater, thus providing for larger DO concentration gradients, BOD is likely to be substantially greater. This indicates that in the southeastern region of CCB, where mixing is minimal and the water column is shallow, the sediments alone could cause the onset of a hypoxic event in the relatively short time period of a few days and must, therefore, be considered a major and probably dominant contributing factor to hypoxia in CCB.

5.2. MISSISSIPPI RIVER BIGHT HYPOXIA

5.2.1. *Relationship between BOD and SRR*

Sediments from the MRB site also had greater changes in dissolved Fe^{2+} than $\sum\text{H}_2\text{S}$ and the Fe^{2+} maximum was near the sediment–water interface. This caused Fe^{2+} to be more responsive to changes in the overlying water DO than $\sum\text{H}_2\text{S}$.

Integrated SRR and BOD values presented in Table III were comparable to previously measured rates in the area (SRR 12–14 $\text{mmol m}^{-2} \text{day}^{-1}$; Lin and Morse, 1991; Canfield, 1994; BOD 19–56 $\text{mmol m}^{-2} \text{day}^{-1}$ for slightly hypoxic MRB locations; Morse and Rowe, 1999). SEOD was calculated as described in the CCB discussion. The ratio of SEOD to BOD for the MRB sediments at this site was ~ 1 .

5.2.2. *Iron reduction*

The concentration of HCl-extractable iron in MRB-region sediments, as measured extensively by Lin and Morse (1991), averages $230 \pm 23 \mu\text{mol g dw}^{-1}$. In these sediments the high concentration of reactive iron-oxide minerals may be responsible for the low concentration of $\sum\text{H}_2\text{S}$ and bacterial reduction of iron oxides may also contribute to the extremely high concentrations of dissolved Fe^{2+} .

5.2.3. *Benthic induction of hypoxia*

The thickness of the hypoxic bottom layer at the MRB is often ~ 3 m (DiMarco, 2005, personal communication) and the rate of BOD at MRB is approximately twice that of the CCB (Table III). Consequently, the time for onset of hypoxia in a closed system would be approximately 20 days. The result appears to be reasonable given that Eldridge and Morse (2002) estimated, using a coupled bathy-pelagic numerical model, that in the “dead zone” of the Louisiana shelf (Rabalais et al., 2002) about 60% of the DO consumption producing hypoxic conditions was due to BOD.

5.3. COMPARISONS BETWEEN THE MRB AND THE CCB STUDY LOCATIONS

The CCB and MRB sediments demonstrated significantly ($p < 0.05$) different dissolved Fe^{2+} and $\sum\text{H}_2\text{S}$ dynamics in microcosm studies. Maximum $\sum\text{H}_2\text{S}$ values were greater at the CCB sites compared to the MRB sites and the CCB maximum SRR were almost double those from the MRB. However, the opposite was true for the Fe^{2+} concentrations. This may be attributed to differences in the amount of available iron-oxides where MRB had $230 \pm 23 \mu\text{mol g dw}^{-1}$ and CCB had $10\text{--}40 \mu\text{mol g dw}^{-1}$. At both sites maximum dissolved Fe^{2+} concentrations were greater than dissolved $\sum\text{H}_2\text{S}$. Calculations of estimated induction of hypoxic conditions by the sediments for CCB were less (~ 6 days) than those at the MRB (~ 20 days), indicating that the sediment biogeochemistry may play a more important role in producing hypoxia at CCB which has a thinner layer of hypoxic water.

6. Conclusions

This study of the CCB and MRB sediments demonstrated significantly ($p < 0.05$) different dissolved Fe^{2+} and $\sum\text{H}_2\text{S}$ dynamics. No significant differences ($p < 0.05$) between experimental microcosms and field monitoring cores with respect to $\sum\text{H}_2\text{S}$ and the high concentrations of Fe^{2+} indicated that CSV microelectrodes were an appropriate methodology to gain insight into the natural dynamics of these reduced species in sediments overlain by hypoxic bottom waters. Reduced porewater Fe^{2+} was greater than porewater $\sum\text{H}_2\text{S}$ at both sites clearly demonstrating that iron reduction/oxidation needs to be considered in addition to the traditionally considered sulfides and may be of substantial interest for future studies aiming to understand the role of benthic–pelagic coupling in seasonally hypoxic waters. Results also indicated that sediments can be responsible for the induction of hypoxic conditions in shallow bays and estuaries.

Acknowledgements

Funding for this work provided by the Louis and Elizabeth Scherck Chair held by John Morse at Texas A&M University. We thank Andy Hebert, Megan Singer, Craig Aumack, and Mark McCarthy for their aid in sample collection and laboratory analyses. We thank contributors from the University of Texas Marine Science Institute, Wayne Gardner, Paul Montagna, and Ken Dunton, for their gracious hospitality and assistance in providing both visiting scientist privileges and laboratory/lodging accommodations.

References

- Aller R. C. (1980) Diagenetic processes near the sediment – water interface of Long Island Sound. II. Fe and Mn, *Adv. Geophys.* **22**, 351–415.
- Berner R. A. and Westrich J. T. (1985) Bioturbation and the early diagenesis of carbon and sulfur, *Am. J. Sci.* **285**, 193–206.
- Brendel P. J. (1995) *Development of a Mercury Thin Film Voltammetric Microelectrode for the Determination of Biogeochemically Important Redox Species in Porewaters of Marine and Freshwater Sediments*, Ph.D. thesis, University of Delaware, Newark.
- Brendel P. J. and Luther G. W. III (1995) Development of a gold amalgam voltammetric microelectrode for the determination of dissolved Fe, Mn, O₂, S(-II) porewaters of marine and freshwater sediments, *Environ. Sci. Technol.* **29**, 751–761.
- Buzzelli C. P., Luettich R. A., Powers S. P., Peterson C. H., McNinch J. E., Pinckney J. L. and Paerl H. W. (2002) Estimating the spatial extent of bottom-water hypoxia and habitat degradation in a shallow estuary, *Mar. Ecol. Prog. Ser.* **230**, 103–112.
- Canfield D. E. (1994) Factors influencing organic carbon preservation in marine sediments, *Chem. Geol.* **114**, 315–329.
- Canfield D. E., Raiswell R., Westrich J. T., Reaves C. M. and Berner B. (1986) The use of chromium reduction in the analysis of reduced inorganic sulfur in sediments and shales, *Chem. Geol.* **54**, 149–155.
- Cline J. D. (1969) Spectrophotometric determination of hydrogen sulfide in natural waters, *Limnol. Oceanogr.* **14**, 454–458.
- Cooper D. C. and Morse J. W. (1996) The chemistry of Offatts Bayou, Texas: a seasonally highly sulfidic basin, *Estuaries* **19**, 595–611.
- Dauer D. M. and Ranasinghe J. A. (1992) Effects of low dissolved oxygen events on the macrobenthos of the lower Chesapeake Bay, *Estuaries* **15**, 384–391.
- Eldridge P. M. and Morse J. W. (2002) A model for changes in sediment and water column biogeochemistry in response to seasonal hypoxic/anoxic conditions beneath the Mississippi River plume. *Abstracts 6th International Symposium on the Chemistry of the Earth's Surface*, Honolulu, Hawaii.
- Froelich P. N., Klinkhammer G. P., Bender M. L., Luedtke N. A., Heath G. R., Cullen D., Dauphin P., Hammond D., Hartman B. and Maynard V. (1979) Early oxidation of organic matter in pelagic sediments of the eastern equatorial Atlantic: Suboxic diagenesis, *Geochim. Cosmochim. Acta* **43**, 1075–1090.
- Harper D. E., McKinney L. D., Salzar R. R. and Case R. J. (1981) The occurrence of hypoxic bottom water off the upper Texas coast and its effect on the benthic biota, *Contr. Mar. Sci.* **24**, 53–79.
- Jørgensen B. B., Bang M. and Blackburn T. H. (1990) Anaerobic mineralization in marine sediments from the Baltic Sea-North Sea Transition, *Mar. Ecol. Prog. Ser.* **59**, 39–54.
- Jørgensen B. B. (1980) Seasonal oxygen depletion in the bottom waters of a Danish fjord and its effect on the benthic community, *Oikos* **34**, 68–76.
- Jørgensen B. B. (1978) A comparison of methods for the quantification of bacterial sulfate reduction in coastal marine sediments. Measurement with radiotracer techniques, *J. Geomicrobiol.* **1**, 11–28.
- Jørgensen B. B. (1977) The sulfur cycle of a coastal marine sediment (Limfjorden, Denmark), *Limnol. Oceanogr.* **22**, 814–832.
- Kana T. M., Darkangelo C., Hunt M. D., Oldham J. B., Bennett G. E. and Cornwell J. C. (1994) Membrane inlet mass spectrometer for rapid high-precision determination of N₂, O₂, and Ar in environmental water samples, *Anal. Chem.* **66**, 4166–4170.

- Kristiansen K. D., Kristensen E. and Jensen M. H. (2002) The influence of water column hypoxia on the behavior of manganese and iron in sandy coastal marine sediment, *Estuarine Coastal Shelf Sci.* **55**, 645–654.
- Lavrentyev P. J., Gardner W. S. and Yang L. (2000) Effects of the zebra mussel on microbial composition and nitrogen dynamics at the sediment–water interface in Saginaw Bay, Lake Huron, *Aquatic Microbiol. Ecol.* **21**, 187–194.
- Lin S. and Morse J. W. (1991) Sulfate reduction and iron sulfide mineral formation in Gulf of Mexico anoxic sediments, *Am. J. Sci.* **290**, 55–89.
- Luther G. W. III, Ma S., Trouwborst R., Glazer B., Blickley M., Scarborough R. W. and Mensinger M. G. (2004) The roles of anoxia, H₂S and storm events in fish kills of dead-end canals of Delaware inland bays, *Estuaries* **27**, 551–560.
- Luther G. W. III, Brendel P. J. and Lewis B. L. (1998) Simultaneous measurement of O₂, Mn, Fe (–I) and S(–II) in marine porewaters with a solid-state voltammetric microelectrode, *Limnol. Oceanogr.* **43**, 325–333.
- Morse J. W. and Rowe G. T. (1999) Benthic biogeochemistry beneath the Mississippi river plume, *Estuaries* **22**, 206–214.
- Morse J. W. and Rickard D. (2004) The influence of sedimentary acid volatile sulfide (AVS) chemical dynamics on toxic metal bioavailability, *Environ. Sci. Technol.* **38**, 131A–136A.
- Rabalais N. N., Wiseman W. J. and Turner R. E. (1994) Comparison of continuous records of near-bottom dissolved oxygen from the hypoxic zone along the Louisiana coast, *Estuaries* **17**, 850–861.
- Rabalais N. N., Turner R. E. and Wiseman W. J. (2002) Gulf of Mexico hypoxia, A.K.A. “The dead zone”, *Annu. Rev. Ecol. Syst.* **33**, 235–263.
- Ritter C. and Montagna P. A. (1999) Seasonal hypoxia and models of benthic response in a Texas bay, *Estuaries* **22**, 7–20.
- Roden E. E. and Tuttle J. H. (1992) Sulfide release from estuarine sediments underlying anoxic bottom water, *Limnol. Oceanogr.* **37**, 725–738.
- Rowe G. T. (2001) Seasonal hypoxia in the bottom water off the Mississippi river delta, *J. Environ. Qual.* **30**, 281–290.
- Sell K. S. (2003) *The Temporal Influences of Seasonal Hypoxia on Sediment Biogeochemistry in Coastal Sediments*, M.S. thesis, Texas A&M University, College Station.
- Stow C. A., Qian S. S. and Craig J. K. (2005) Declining threshold for hypoxia in the Gulf of Mexico, *Environ. Sci. Technol.* **39**, 716–723.
- Thamdrup B. (2000) Bacterial manganese and iron reduction in aquatic sediments, *Adv. Microb. Ecol.* **16**, 41–84.
- Thamdrup B., Henrik F. and Jørgensen B. B. (1994) Manganese, iron, and sulfur cycling in a coastal marine sediment, Aarhus Bay, Denmark, *Geochim. Cosmochim. Acta* **58**, 5115–5129.
- Theberge S. and Luther G. W. III (1997) Determination of the electrochemical properties of a soluble aqueous FeS species present in sulfide solutions, *Aquatic Geochem.* **3**, 191–211.
- Thiermann F., Vismann B. and Giere O. (2000) Sulfide tolerance of marine nematode *Oncholaimus campylocercoides* – a result of internal sulfide formation? *Mar. Ecol. Prog. Ser.* **193**, 251–259.
- Wilkin R. T. and Barnes H. L. (1997) Pyrite formation in an anoxic estuarine basin, *Am. J. Sci.* **297**, 620–650.